Insight into the chromophore of rhodopsin and its Meta-II photointermediate by 19F solid-state NMR and chemical shift tensor calculations

Brinkmann, A.; Sternberg, U.; Bovee-Geurts, P.H.M.; Fernández Fernández, I.; Lugtenburg, J.; Kentgens, A.P.M.; Grip, W.J. de

Check for updates

Insight into the chromophore of rhodopsin and its Meta-II photointermediate by ^{19}F solid-state NMR and chemical shift tensor calculations†

Andreas Brinkmann, [ID] *[a] Ulrich Sternberg,[b] Petra H. M. Bovee-Geurts,[c] Isabelle Fernández Fernández,‡[d] Johan Lugtenburg,[d] Arno P. M. Kentgens [ID] [e] and Willem J. DeGrip [ID] *[cd]

[19]F nuclei are useful labels in solid-state NMR studies, since their chemical shift and tensor elements are very sensitive to the electrostatic and space-filling properties of their local environment. In this study we have exploited a fluorine substituent, strategically placed at the C-12-position of 11-*cis* retinal, the chromophore of visual rhodopsins. This label was used to explore the local environment of the chromophore in the ground state of bovine rhodopsin and its active photo-intermediate Meta II. In addition, the chemical shift and tensor elements of the chromophore in the free state in a membrane environment and the bound state in the protein were determined. Upon binding of the chromophore into rhodopsin and Meta II, the isotropic chemical shift changes in the opposite direction by +9.7 and −8.4 ppm, respectively. An unusually large isotropic shift difference of 35.9 ppm was observed between rhodopsin and Meta II. This partly originates in the light-triggered 11-*cis* to all-*trans* isomerization of the chromophore. The other part reflects the local conformational rearrangements in the chromophore and the binding pocket. These NMR data were correlated with the available X-ray structures of rhodopsin and Meta II using bond polarization theory. For this purpose hydrogen atoms have to be inserted and hereto a family of structures were derived that best correlated with the well-established ^{13}C chemical shifts. Based upon these structures, a 12-F derivative was obtained that best corresponded with the experimentally determined ^{19}F chemical shifts and tensor elements. The combined data indicate strong changes in the local environment of the C-12 position and a substantially different interaction pattern with the protein in Meta II as compared to rhodopsin.

Introduction

Rhodopsin is the visual pigment of the rod photoreceptor cells in the vertebrate retina, which mediate dim-light vision.[1–3] As a member of the membrane protein superfamily of the hepta-helical G protein-coupled receptors, rhodopsin is specialized for activation by photons in such a way that its ligand is the photosensory element (chromophore) that has become covalently bound to the apoprotein, opsin. The ligand is a vitamin A derivative, 11-*cis* retinal (Fig. 1), which is attached to Lys-296 in the binding site through formation of a protonated Schiff base.[1,4–7] This local charge is stabilized by a nearby located soft counterion formed by a H-bonded network concentrated around a glutamate residue of opsin (Glu-113).[8–13] The 11-*cis* isomer acts as a potent inverse agonist of opsin, nearly completely eliminating its basal activity, but light absorption can convert it into the all-*trans* configuration that acts as a full agonist.[2,14] This photo-isomerization of the ligand induces conformational changes in the protein, which are driven by about 35 kcal of photon energy stored in the photoproduct Batho.[15–17] Within several milliseconds these structural transitions culminate in generation of the active state, Meta II, which binds and activates its cognate G protein transducin.[14,18] The active state is characterized by deprotonation of the Schiff base[14,19,20] and by subtle rearrangements in several structural elements like helices V, VI and VII, intracellular loops and the binding site with the

[a] *Metrology, National Research Council Canada, 1200 Montreal Road, Ottawa, Ontario, K1A 0R6, Canada. E-mail: Andreas.Brinkmann@nrc-cnrc.gc.ca*

[b] *Karlsruhe Institute of Technology, P.O. Box 3640, 76021 Karlsruhe, Germany*

[c] *Department of Biochemistry, UMCN 286, Radboud Institute for Molecular Life Sciences, Radboud University Medical Center, P.O. Box 9101, 6500 HB Nijmegen, The Netherlands. E-mail: Wim.deGrip@radboudumc.nl*

[d] *Leiden Institute of Chemistry, Leiden University, P.O. Box 9502, 2300 RA Leiden, The Netherlands*

[e] *Institute for Molecules and Materials, Radboud University Nijmegen, Heyendaalsweg 135, 6525 AJ Nijmegen, The Netherlands*

† Electronic supplementary information (ESI) available. See DOI: 10.1039/c8cp05886e

‡ Present address: International Flavors & Fragrances, Avda. Felipe Klein 2, 12580 Benicarló (Castellon), Spain.

30174 | *Phys. Chem. Chem. Phys.*, 2018, **20**, 30174–30188

This journal is © the Owner Societies 2018
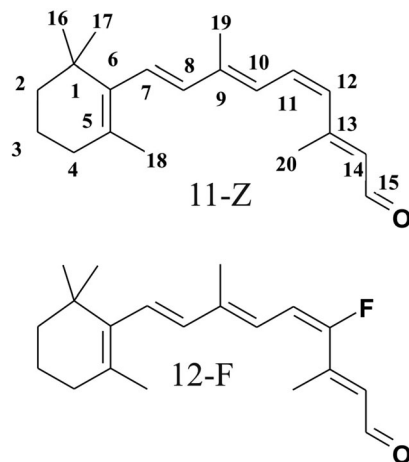
Fig. 1 Chemical structure of 11-*cis* retinal (11-*Z*) and the 12-fluoro derivative used in this study. The structures are shown in the 12-s *trans* conformation, which is dictated by the opsin binding pocket.

ligand in the all-*trans* configuration.[21–31] Meta II decays with a half time of minutes, whereby the all-*trans* retinal is released from the orthosteric binding site and the opsin structure partially reverts to the original rhodopsin conformation.[1,32–35] The availability of crystal structures of rhodopsin, Meta II and opsin presents a major step forward in understanding important elements of the activation mechanism of G protein-coupled receptors.[26] On the other hand, the resolution varies between 2.2 and 3.3 Å,[11,12,24,25,36–38] which implies that atomic details cannot be exactly derived from the electron density. For instance, modeling is used to derive the position of the ligand, and this position is not equivalent to the one obtained by quantum mechanics/molecular dynamics.[12] In addition, the crystal lattice imposes limitations on the 3D conformation of the protein, in particular the more flexible intracellular surface, and may select one that is not the dominant one in the natural aqueous membrane dispersion.[11,12,31,39,40]

Hence it is essential to confront crystal structures with experimental evidence derived from alternative conformational analyses allowing a natural membrane environment. While biochemical and biophysical (ESR, NMR, wide-angle X-ray scattering) data generally qualitatively agree with the structural alterations in the transition from rhodopsin to Meta II as indicated by the crystal structures,[3,10,13,21–23,27,28,35,41,42] quantitative agreement has proven to be difficult to achieve, as yet.[31,43]

Here we present a solid-state NMR approach with fluorine-labeling in combination with computational chemistry. The advantage of the fluorine label as a NMR probe is its high gyromagnetic ratio, large chemical shift range and high sensitivity to its local environment.[44–46] In addition, from the spinning side bands in solid state NMR the principal values of the chemical shift (CS) tensors can be easily derived, which provide additional geometrical information. Prerequisite for drawing sensitive conclusions from the tensor elements is that the orientation of the fluorine CS tensor is known. Fluorine labels have been used before in solution NMR studies on rhodopsin solubilized in detergent micelles to probe its photoactivation. The label was

introduced either by chemical modification of cysteine mutants or by phosphorylation[35,47,48] or by incorporation of fluoro-labeled retinals.[49–53] We have opted for an 11-*cis* retinal analog, since the microenvironment of the rhodopsin ligand is relatively well defined in the crystal structures. A fluorine label at C-12 was selected (Fig. 1) since the C-10–C-13 segment in the chromophore is the trigger point for the photoactivation of rhodopsin[54–61] and reorientation of the chromophore proceeds up to the Meta II state.[13,24,62,63] Furthermore, the ^{19}F-chemical shift at the C-12 position was shown not to be very sensitive to the group at C-15 (free aldehyde or (un)protonated Schiff base),[49,50,52] and in a recent study we showed that photo-activation triggers changes in the vibrational properties of a fluorine label at C-12.[64]

In this report we demonstrate that incorporation of 11-*cis* 12-F-retinal results in a significant positive ligation shift of the chemical shift of the fluorine label, primarily reflected in the δ_{11} and δ_{22} tensor elements, while Meta II exhibits a significant negative ligation shift, primarily reflected in the δ_{33} tensor element. Our subsequent computational studies demonstrate that the isotropic ligation shift and changes of the tensor elements originate in changes of the F–C bond length and the polarizing influence of the microenvironment of the retinal.

Experimental section

Materials

All chemicals were of analytical grade. Detergents were obtained from Anatrace (Maumee, OH, USA). Unmodified 11-*cis* retinal was provided by Dr Rosalie Crouch (Medical University of South Carolina, Charleston, USA) through financial support from NEI.

Synthesis of 12-F retinal

The 12-F derivative was prepared in the 11-*cis* configuration as described before.[65] In this case the C15 precursor was synthesized as a mixture of the all-*trans* and 11-*cis* isomers. The 11-*cis* isomer was isolated by chromatography and extended into the corresponding retinal. The spectral and ^{1}H NMR characteristics of the obtained 11-*cis* 12-F-retinal agreed with published data.[64,65]

Isolation of bovine opsin and regeneration with 11-*cis* retinals

Bovine rod outer segment membranes in the opsin form (opsin membranes) were prepared from fresh, light-adapted cattle eyes as described.[66,67] The regeneration capacity of these preparations was estimated from the A_{280}/A_{500} ratio measured after subsequent incubation with a 3-fold excess of 11-*cis* retinal, whereby a ratio of 2.1 ± 0.1 was taken to represent membranes with a maximal rhodopsin content. Rhodopsin and the 12-fluoro-rhodopsin analog were prepared with opsin membranes showing a regeneration capacity in the range 90–100%. Regeneration and all further manipulations with the pigments were done under dim red light (>620 nm, RG645 longpass filter).

The 12-F analog pigment was generated by incubating a suspension of opsin membranes (50–100 μM opsin in buffer A: 20 mM PIPES, 130 mM NaCl, 5 mM KCl, 2 mM CaCl₂, 0.1 mM EDTA, 1 mM DTE, pH 6.5) with a 2–3 fold molar excess of the

11-*cis* fluororetinal at room temperature. After two hours a small aliquot was assayed for the extent of regeneration by addition of 11-*cis* retinal in a 1/1 molar ratio to the original opsin. Regeneration appeared to be nearly complete and to achieve full regeneration an additional aliquot of the fluoro-retinal was added and the incubation continued overnight at 4 °C. Excess retinal was then converted into the corresponding oxime by addition of an 1 M hydroxylamine solution (pH 6.5) to a final concentration of 10 mM. After cooling in ice and 30 min incubation, the oxime was largely removed by two extractions with 50 mM heptakis-(2,6-di-*O*-methyl)-β-cyclodextrin,[66] which, however, also removes some lipids thereby perturbing the Meta I to Meta II transition. To restore a native lipid/protein ratio, the membrane pellet was dissolved in 20 mM nonylglucoside in buffer A (to *ca.* 50 μM of pigment) by incubation for 1 h on ice. Undissolved material was removed by centrifugation (30 min, 80 000 × g, 4 °C), and the supernatant mixed with a solution of asolectin (100 mg ml^{-1} in 50 mM nonylglucoside in buffer A) to achieve a 50-fold molar excess of asolectin with respect to pigment. After 15 min incubation on ice, detergent was extracted by addition of solid β-cyclodextrin to a slight excess over non-ylglucose and the resulting proteoliposomes isolated by overnight sucrose step-gradient centrifugation at 200 000 × g and 4 °C as described before.[68] The proteoliposome band was recovered from the 20%/45% sucrose interface, diluted with 2 volumes of doubly distilled water, pelleted by centrifugation (60 min, 200 000 × g, 4 °C) and stored in aliquots under Argon in a light-tight container at −80 °C.

UV/vis spectroscopy

The spectral properties of the pigments were determined in micellar solution, by solubilization to about 2.5 μM in 20 mM dodecylmaltoside in buffer A containing 10 mM hydroxylamine. The wavelength of maximal absorbance in the visible region (λ_{max}) was determined as the peak position in the difference spectrum obtained after subtraction of the spectrum after illumination (300 s; 150 W halogen light through a Schott OG530 longpass filter and fiber optics) from the dark state spectrum.

The photoequilibrium obtained after illumination was analysed using the end-on photomultiplier set-up of a Perkin-Elmer Lambda 18 spectrophotometer. Pigment proteoliposomes were suspended to about 30–40 μM of pigment in buffer B (similar to buffer A, but with 20 mM MES as a buffering compound and a pH of 5.0). The sample was maintained at 0 °C in a melting ice bath and illuminated (conditions as above). Aliquots were taken before and after 30 s, 2 min and 4 min of illumination, and spectra were recorded in a cuvette with a 2 mm light path. After 4 min of illumination the proteoliposomes were spun down (20 min, 100 000 × g, 0 °C) and the pellet was frozen in a solid CO_2/alcohol mixture.

Preparation of 12-F rhodopsin and 12-F metarhodopsin II (Meta II)

The 11-*cis* 12-F-retinal derivative (Fig. 1) was prepared and purified as described before.[64,65] All manipulations with rhodopsin were performed under dim red light (Schott RG645 longpass filter)

except for the preparation of Meta II. The rhodopsin 12-F analogue was prepared from opsin and 11-*cis* 12-F-retinal, also as described before,[64] yielding a pigment with its maximal absorbance at 510 ± 2 nm (Fig. 2) in agreement with earlier data.[64,65] In comparison to rhodopsin the Meta I to Meta II transition of 12-F rhodopsin is strongly shifted to a lower pH range.[64] Therefore, 12-F Meta II was generated by illumination of 12-F rhodopsin in proteoliposomes at a pH of 5.0, where close to maximal conversion to Meta II can be realized.[64] Since the decay of Meta II is strongly reduced at lower temperature, illumination was performed at 0 °C, where the half-life of Meta II is several hours. Under the selected conditions maximal conversion to 12-F Meta II could be achieved after 4 min of illumination (Fig. 2). Based upon the pH dependence of the 12-F Meta I to Meta II transition and the absorbance shift[64,69] it was estimated that the photoproduct consisted of about 10% remaining rhodopsin, 20% Meta I and 70% Meta II. Meta II can be stabilized by freezing below −13 °C (260 K)[70] and, after filling the rotor with the Meta II proteolipo-somes by centrifugation at 0 °C, the rotor was stored at −80 °C.

Solid-state NMR spectroscopy

Varian 4 mm rotors were used, where the standard Vespel spacer and endcap had been replaced by ones machined from Kel-F. All subsequent manipulations were performed in the dark or under dim red light (Schott RG645 longpass filter). The rotors were filled with pigment proteoliposomes by centrifugal force (120 min, 30 000 × g, 0 °C).[9] Per rotor about 300 nmoles (12 mg) of pigment was applied. The frozen pellet of the Meta II sample, generated as described above, was directly applied into the centrifuge tube insert, and allowed to melt during centri-fugation, thereby pelleting the released membranes. The filled rotors were stored at −80 °C for maximally two days before the NMR analysis was started.
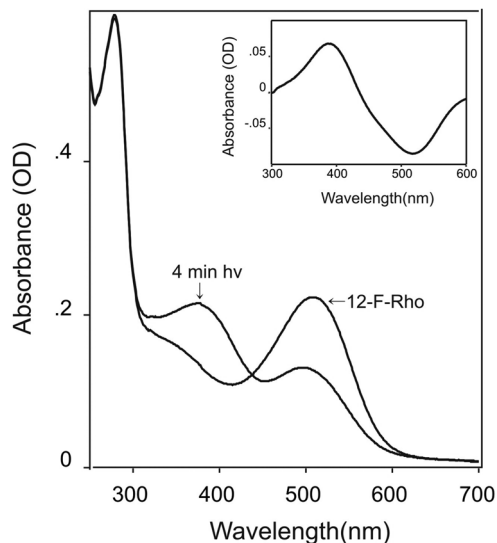

Fig. 2   UV/vis spectra of 12-F rhodopsin in proteoliposome suspension before (12-F-Rho) and after four min of illumination (4 min hν). The inset presents the difference between these spectra, demonstrating that the major photoproduct is Meta II (385 nm absorbance band).

All experiments were performed on either a Varian Infinity or VNMRS console at a static magnetic field of 14.1 T, employing a Chemagnetics 4 mm HFXY quadruple resonance probehead. The top and the bottom of the magnet bore were covered by blackout curtains to prevent any light from reaching the sample during the NMR experiments. The ^{19}F cross-polarization (from ^{1}H) magic-angle-spinning (CP-MAS) experiments[71] were performed at ^{1}H and ^{19}F Larmor frequencies of 600 and 564.5 MHz, respectively, using spinning frequencies of 10 or 12 kHz and a ^{19}F Hahn echo[72] of two rotational periods before ^{19}F signal detection under proton decoupling. The ^{19}F spectra were referenced to CCl$_3$F *via* the ^{13}C chemical shift of the Adamantane resonance following the IUPAC recommendations.[73,74] All ^{19}F experiments were setup using a powdered sample of Fmoc-(4-F)-Phe-OH at room temperature. The calibration of the variable temperature (VT) controller using a sample of lead nitrate (Pb(NO$_3$)$_2$)[75,76] showed that a readout temperature of -80 °C used in our low-temperature experiments on rhodopsin corresponds to sample temperatures of -71.5 °C at 12 kHz MAS frequency and -74.8 °C at 10 kHz MAS frequency, hence well below the temperature where Meta II starts to decay.

The ^{19}F CP-MAS spin-echo experiments on the sample of 11-*cis* 12-F-retinaloxime in liposomes were performed at 10 and 12 kHz MAS frequency, at a sample temperature of -74.8 and -71.5 °C, respectively, utilizing a 90° proton pulse of 3.1 μs, and a ^{19}F 180° pulse of 8 μs. The nutation frequency of the proton rf field during CP was given by 40 kHz and the rf field on the ^{19}F was adjusted to fulfill the (+1) Hartman–Hahn sideband matching condition.[71] XiX proton decoupling[77] with a nutation frequency of 58 kHz was applied during ^{19}F signal detection. In total 5120 transients were accumulated with a relaxation delay of 10 s between each transient. An exponential apodization function with a width of 500 Hz was applied before Fourier transformation of the ^{19}F time domain signal.

The experiments with 12-F rhodopsin were also performed at 10 and 12 kHz MAS frequency, at a sample temperature of -74.8 and -71.5 °C, respectively, and the same experimental parameters were used as for the 11-*cis* 12-F-retinoxime sample. The number of total accumulated transients was 56 432 and 15 984 for the ^{19}F CP-MAS spin echo experiments at 10 and 12 kHz MAS frequency, respectively, using a relaxation delay of 5 s. Exponential apodization with a width of 500 Hz was again applied to the time domain signal.

The CP-MAS experiments with illuminated 12-F rhodopsin were solely performed at a MAS frequency of 12 kHz and a sample temperature of -71.5 °C. The ^{1}H 90° and ^{19}F 180° pulses were given by 3 and 8 μs, respectively. The proton rf field during the cross-polarization was set to 53 kHz and the ^{19}F rf field was adjusted to match the (-1) Hartman–Hahn sideband condition. The nutation frequency of the XiX decoupling during ^{19}F signal detection was given by 53 kHz. 14 048 transients with a relaxation delay of 5 s were recorded, and an exponential apodization function with a width of 500 Hz was again applied before Fourier transformation.

Analysis of solid-state NMR spinning-sideband patterns

The experimental MAS sideband patterns of the ^{19}F chemical shift interaction were fitted to calculations to obtain the 3 principal components of the chemical shift tensor. We chose to present our results using both the Haeberlen and Maryland conventions[73,78,79] since both have their merits when discussing results from experiments and theoretical calculations. In the Haeberlen convention[73,78] the three principal components in the deshielding convention are labeled δ_{XX}, δ_{YY} and δ_{ZZ} and ordered according to $|\delta_{ZZ} - \delta_{iso}| \geq |\delta_{XX} - \delta_{iso}| \geq |\delta_{YY} - \delta_{iso}|$, where the isotropic chemical shift is given by $\delta_{iso} = (\delta_{XX} + \delta_{YY} + \delta_{ZZ})/3$. In addition, the anisotropic chemical shift δ_{aniso} and asymmetry parameter η of the chemical shift anisotropy (CSA) are defined as $\delta_{aniso} = \delta_{ZZ} - \delta_{iso}$ and $\eta = (\delta_{YY} - \delta_{XX})/\delta_{aniso}$, respectively. On the other hand, in the Maryland convention[73,79] the three principal components are labeled δ_{11}, δ_{22} and δ_{33} and are ordered according to $\delta_{11} \geq \delta_{22} \geq \delta_{33}$. The isotropic chemical shift δ_{iso}, the span Ω and skew κ are given by $\delta_{iso} = (\delta_{11} + \delta_{22} + \delta_{33})/3$, $\Omega = \delta_{11} - \delta_{33}$ and $\kappa = 3(\delta_{22} - \delta_{iso})/\Omega$. The Maryland convention is useful when discussing the chemical shift tensor as a whole, while the Haeberlen convention is more applicable when discussing the CSA principal tensor values separately from the isotropic chemical shift. Below we will report the three principal components δ_{11}, δ_{22} and δ_{33} as well as δ_{iso}, δ_{aniso}, η, Ω and κ. The spinning-sideband amplitudes for a single crystallite orientation are calculated by discrete Fourier transformation of the signal amplitudes obtained by evolution under the chemical shift interaction over one rotational period.[80] The final spinning-sideband manifold is obtained by powder averaging using the octant Lebedev set containing 109 pairs of Euler angles.[81] The experimental ^{19}F spectra were fitted in a single step to the calculated sideband manifold, hence fitting parameters included not only the parameters (δ_{iso}, δ_{aniso}, η), but also the parameters describing the shape of the centerband line according to a linear combination of a Gaussian and Lorentzian line shape (overall scaling, width, fraction Lorentzian). Hence, a total of 6 fitting parameters were used for each sample component. Experimental results obtained at different spinning frequencies were simultaneously fitted. We obtained the 68.27% confidence interval, corresponding to an error of plus/minus one standard deviation for a normal distribution, for δ_{aniso} and η, in a separate step by calculating the sum-squared deviation S between the experimental and calculated integrated sideband amplitudes for a series of different values for either δ_{aniso} or η, where the other fitting parameters were optimized as to minimize S in each case. The confidence interval is determined by the set of values for either δ_{aniso} or η for which $S \leq S_{min}\{1 + F^{\alpha}_{1,n-p}/(n - p)\}$, where S_{min} is the sum-squared deviation minimized by optimizing all fitting parameters, n is the number of integrated sideband amplitudes used in the fit, p is the total number of fitting parameters, $\alpha = 0.3173$ and $F^{\alpha}_{p_1,p_2}$ is the upper α probability point of the F distribution with p_1 and p_2 degrees of freedom.[82,83] The error of δ_{aniso} is determined in an analogous manner from the direct line shape fitting of the spinning sideband manifold. The errors for Ω, κ, δ_{11}, δ_{22} and δ_{33} were estimated by error propagation.

Computational modeling and NMR tensor calculations by bond polarization theory (BPT)

The bond polarization theory (BPT) works with localized bond contributions and the influence of changes of the structure and

charge distribution on molecular properties can be readily separated and discussed. In this investigation the BPT is used for atomic partial charges[84] and ^{13}C and ^{19}F chemical shifts.[46,85] For the ^{19}F chemical shift the BPT equation has a simple form since only the polarization of the F–C bond has to be discussed. Eqn (1) gives the BPT expression for the chemical shift tensor $\boldsymbol{\delta}$ in the bond coordinate system of the F–C bond:

$$\delta_{\alpha\beta} = n\delta_{\alpha\beta}^{F-C} + n^2 A_{\alpha\beta}^{F-C}(\langle\chi_F|\hat{V}|\chi_F\rangle - \langle\chi_C|\hat{V}|\chi_C\rangle) \qquad (1)$$

In the bond coordinate system (the z-axes are pointing into bond direction) the chemical shift tensor is regarded as diagonal with the principal components $\{\delta_{xx}, \delta_{yy}, \delta_{zz}\}$ (the discussion of eqn (1) is given in terms of chemical shift and in this case we have to add -93.68 ppm as sum of the ^{19}F inner shell contribution of -306.3 ppm[86] and a reference shielding of 212.62 ppm, see ref. 46). The principal components are calculated as a sum of two terms: a bond tensor δ^{F-C} and a second term describing the change of the nuclear shielding by polarization. The bond tensor stands for a bond with the configuration weight $n = 1.0$ with no polarizing charges in its surrounding.

The principal components of this CS bond tensor are given in Table 1 and in CS calculations this bond tensor is scaled by the configuration weight of the bond n. The introduction of n means that the bonds are not treated as strictly localized but bond electrons can occupy anti-bond states in other bond configurations. An empirical relation connects the configuration weight to valence of the bond and to the bond length.[87,88] In this BPT description the bond tensor contains also the shift contributions of the three fluorine lone pair orbitals.

The term in brackets in eqn (1) is called polarization energy and is calculated from the potentials V of the charges q in the surrounding of the F–C bond and from the fluorine hybrid orbitals χ_F and the carbon hybrid orbitals χ_C forming the bond. Since the influence of potentials q/r get weaker with increasing distance r only charges in the vicinity of the F–C bond have a large influence. To get the polarizing influence on the chemical shift the polarization energy is multiplied by the tensor $\boldsymbol{A}^{F-C}$ with the dimension ppm/energy (Table 1). These principal components can be (in good approximation) assigned to the bond coordinate system in the following way: component yy perpendicular to the carbon π system, component xx within the π plane and zz in F–C bond direction. The polarization energy is a scalar but the tensor $\boldsymbol{A}^{F-C}$ can have very different elements even with different signs and therefore the polarizing influence in different directions is highly anisotropic. Since both tensors $\boldsymbol{\delta}^{F-C}$ and $\boldsymbol{A}^{F-C}$ are diagonal with respect to the bond coordinate system the final result of eqn (1) will be diagonal in this coordinate system as well. Only through-space shieldings of other bonds could contribute off-diagonal elements but these contributions are neglected in the framework of the BPT.

The problem of quantum chemical CS calculations is the need for precise structures. Minute bond length changes can cause large changes in chemical shifts and even X-ray structures are not precise enough. The next problem of the X-ray investigations is that in the case of the rhodopsin structures no proton positions are refined. Starting with the X-ray structure of the dark adapted rhodopsin (PDB 1U19) by Okada *et al.*[12] and the structure of the light activated form (PDB 4A4M) by Deupi *et al.*,[36] protons are substituted and possible van der Waals contacts where healed out by short MD simulations (for the complete modeling protocol see the ESI†).

Starting from the BPT equations derivatives of the chemical shifts with respect to Cartesian coordinates have been developed[89] and these CS derivatives allow geometry optimizations with chemical shifts as constraints. It is possible to derive pseudo-energies from the differences of calculated and experimental chemical shifts and the derivatives of these pseudo-energies are CS pseudo-forces that are needed to drive the geometry optimizations. The CS pseudo-energies are added to the regular energies of the COSMOS-NMR force field.[90,91] The COSMOS-NMR force field has the possibility to work with several forms of NMR constraints and it has been applied to protein structure investigations using ^{13}C and ^{15}N chemical shifts.[85] This opens the possibility to refine the structure of the retinal molecule and its binding pocket within the retinal protein. We used literature data for the ^{13}C chemical shifts of the retinal as collected by Frähmke *et al.*[92] as constraints for a global minimum search of both retinal forms. Since gradient procedures for the minimization always run into the next local minimum we refine a large library of more than 1000 MD snapshots and selected the 20 best fitting structures as final result. As criterion we used the CS pseudo energy of the retinal (for details see ESI†). The proton of C12 of retinal was converted into a fluorine and the geometry of the fluorinated compounds was geometry optimized to adjust the C–F bond lengths. Assuming that the fluorination has only a minor influence on the structure these models where used for fluorine tensor calculation. To adjust the retinal structure and its binding surrounding to the fluorination we geometry optimized the models using the experimental isotropic ^{19}F chemical shifts as constraints.

A better way to refine the fluorinated structure would be to search again for a global minimum by using a large library of structures as starting point. But since we had only one experimental NMR constraint we cannot exclude abnormal structures that give the right CS value (see ESI†).

Results

F-NMR analysis of Fmoc-[4-F]-L-phenylalanine-OH

In order to setup optimal conditions and validate the ^{19}F CP-MAS experiments we first analyzed a sample of powdered Fmoc-[4-F]-L-phenylalanine-OH (Fmoc-[4-F]-L-Phe). The results we obtained for

Table 1 Components of the ^{19}F CS bond tensor $\boldsymbol{\delta}^{F-C}$ and the CS polarization tensor $\boldsymbol{A}^{F-C}$. The tensors are assumed to be diagonal in the bond coordinate system with the zz component in F–C direction, the yy component perpendicular to the π plane of the sp^2 carbon and xx within the π plane

Component	xx	yy	zz
^{19}F CS bond tensor [ppm]	-76.98	-203.50	-117.18
CS polarization tensor $\boldsymbol{A}^{F-C}$ [ppm Hartree^{-1}]	-1393.1	-2110.8	450.8

30178 | *Phys. Chem. Chem. Phys.*, 2018, **20**, 30174–30188

This journal is © the Owner Societies 2018

the chemical shift principal components are shown in Table 2. We found isotropic and anisotropic chemical shifts of δ_{iso} = −113.43 ± 0.01 ppm and δ_{aniso} = 61.0 ± 0.5 ppm with an asymmetry parameter of η = 0.74 ± 0.02, corresponding to a span and skew of Ω = 114.0 ± 1.0 ppm and κ = −0.21 ± 0.01, respectively. These values are very close to the δ_{iso} = −110.8 ppm, δ_{aniso} = 58.9 ppm and η = 0.74, reported for the close analog [4-F]-L-Phe by the group of Ulrich.[93] This validates our set-up for the subsequent ^{19}F-NMR studies reported below.

F-NMR analysis of free 11-*cis* 12-F retinal in liposomes

The F-NMR properties of the free ligand were determined for the oxime derivative, since the type of headgroup (free carbonyl or amine derivative) does hardly influence the chemical shift of the 12-F substituent,[49,50,52] and the oxime is much less prone to oxidation and side reactions with lipids. The 11-*cis* 12-F-retinoxime was prepared by addition of 11-*cis* 12-F-retinal, dissolved in DMF, to a suspension of asolectin in buffer A, containing 50 mM hydroxylamine, at a molar ratio of lipid to retinoid of about 5 to 1. The liposomes were then pelleted by centrifugation and subsequently packed into the rotor as described above.

NMR analysis of the ^{19}F CP-MAS spectra shown in Fig. 3 resulted in the data presented in Tables 2 and 3. We found an isotropic and anisotropic chemical shift of δ_{iso} = −104.7 ± 0.2 ppm and δ_{aniso} = 46.2 ± 1.2 ppm together with an asymmetry parameter of η = 0.59 ± 0.09. These values correspond to a span of Ω = 83.0 ± 2.9 ppm and a skew of κ = −0.34 ± 0.08. The isotropic and anisotropic shifts are slightly different but close to the ones found for Fmoc-[4-F]-L-Phe (Table 2) and for other aromatic fluorine sites in amino acids.[93] The isotropic shift agrees quite well with the value of −107 ppm reported for 11-*cis* 12-F-retinal in CDCl$_3$ or CD$_2$Cl$_2$ solution.[49,94] The ^{19}F resonance in 11-*cis* 12-F-retinoxime has a linewidth of 4.3–4.6 kHz, much larger than the 0.4 kHz of Fmoc-[4-F]-L-Phe (Table 2), indicating that the 11-*cis* 12-F-retinoxime molecules in the liposomes are not isotropic but enjoy some conformational freedom and experience a range of different environments resulting in a spread of chemical shifts.

F-NMR analysis of 12-F rhodopsin

In order to obtain ^{19}F spectra of 12-F rhodopsin in the dark state, the sample was brought from storage in dry-ice into the magnet under dim red light (Schott RG645 longpass filter). The resulting CP-MAS fluorine spectra obtained at 10 and 12 kHz spinning frequency are shown in Fig. 4. The linewidth of about 1.8 kHz indicates a well-ordered conformation of the chromophore in 12-F rhodopsin in contrast to the case of the free 11-*cis* 12-F-retinoxime in liposomes. From the ^{19}F spinning-sideband pattern we were able to derive an isotropic and anisotropic chemical shift of δ_{iso} = −95.00 ± 0.06 ppm and δ_{aniso} = 53.3 ± 0.9 ppm together with an asymmetry parameter of η = 0.82 ± 0.03 (Table 2), corresponding to a span and skew of Ω = 101.7 ± 2.0 ppm and κ = −0.15 ± 0.03, respectively. The isotropic chemical shift of the 12-F site exhibits a significant ligation shift of +9.7 ppm in 12-F rhodopsin relative to the free 11-*cis* 12-F-retinoxime (Table 3). This isotropic shift and ligation shift are

Table 2 Experimental and calculated results of ^{19}F chemical shift tensors[a]

Sample	Component	Linewidth[b] [Hz]	Fraction Lorentzian[b] [%]	Haeberlen			Maryland		$\delta_{11} \geq \delta_{22} \geq \delta_{33}$		
				δ_{iso} [ppm]	δ_{aniso} [ppm]	η	Ω [ppm]	κ	δ_{11} [ppm]	δ_{22} [ppm]	δ_{33} [ppm]
Experiments											
Fmoc-[4F]-Phe-OH		384^c/407^e	29^c/27^e	−113.43 ± 0.01	61.0 ± 0.5	0.74 ± 0.02	114.0 ± 1.0	−0.21 ± 0.01	−52.4 ± 0.5	−121.5 ± 0.5	−166.4 ± 0.6
11-*cis* 12-F-retinoxime		4365^c/4624^d	62^c/38^d	−104.7 ± 0.2	46.2 ± 1.2	0.59 ± 0.09	83.0 ± 2.9	−0.34 ± 0.08	−58.4 ± 1.2	−114.2 ± 2.1	−141.4 ± 2.3
12-F rhodopsin (dark state)		1837^c/1785^d	85^c/73^d	−95.00 ± 0.06	53.3 ± 0.9	0.82 ± 0.03	101.7 ± 2.0	−0.15 ± 0.03	−41.7 ± 0.9	−99.9 ± 0.9	−143.4 ± 1.2
12-F rhodopsin (illuminated)	Meta II	2785^d	100^d	−130.9 ± 0.1	54.0 ± 4.5	1.00 (+0, −0.16)	108.1 ± 9.2	0.00 ± 0.06	−76.8 ± 4.5	−130.9 ± 2.2	−184.9 ± 5.0
	Liberated retinal	3273^d	15^d	−122.5 ± 0.1	50.1 ± 4.4	0.87 (+0.13, −0.24)	97.0 ± 9.8	−0.10 ± 0.15	−72.4 ± 4.4	−125.6 ± 4.6	−169.4 ± 6.2
Calculations											
12-F rhodopsin (dark state)	Glu181 protonated			−114.0	60.0	0.67	110.1	−0.27	−54.0	−124.0	−164.1
12-F rhodopsin (dark state)	Glu181 unprotonated			−110.6	63.3	0.49	110.5	−0.44	−47.3	−126.7	−157.8
12-F rhodopsin (illuminated)	Meta II			−125.6	−62.1	0.77	117.2	0.18	−70.5	−118.5	−187.7

^{a} Errors are presented as standard deviation, calculated as explained in the Experimental section. ^{b} Linewidth of the centerband and fraction Lorentzian resulting from the lineshape fitting. ^{c} At 10 kHz MAS frequency. ^{d} At 12 kHz MAS frequency. ^{e} At 13 kHz MAS frequency.
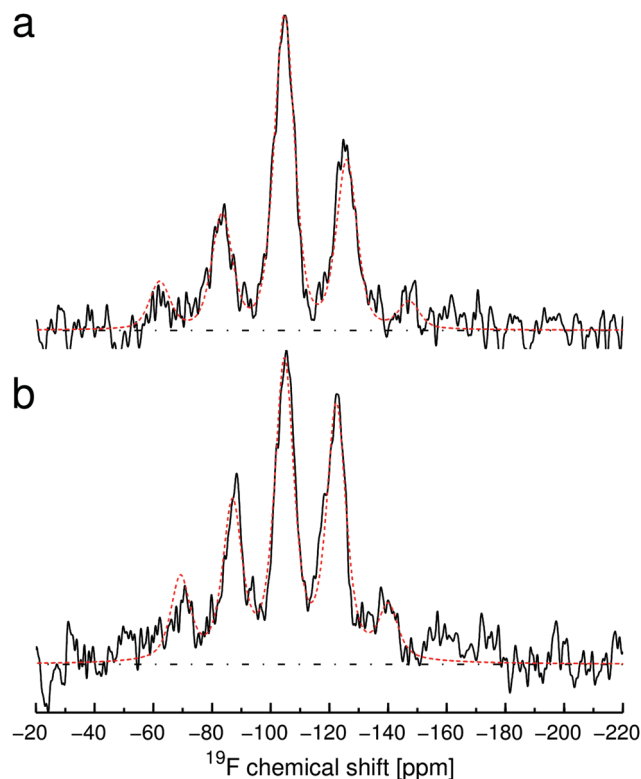
Fig. 3 Solid lines: experimental ^{19}F CP-MAS spectra of 11-*cis* 12-F-retinoxime in asolectin liposomes. Red dashed lines: best-fit results from fitting the chemical shift tensor components. The sample spinning frequency is given by (a) 12 kHz and (b) 10 kHz. The dashed dotted line indicates the baseline.
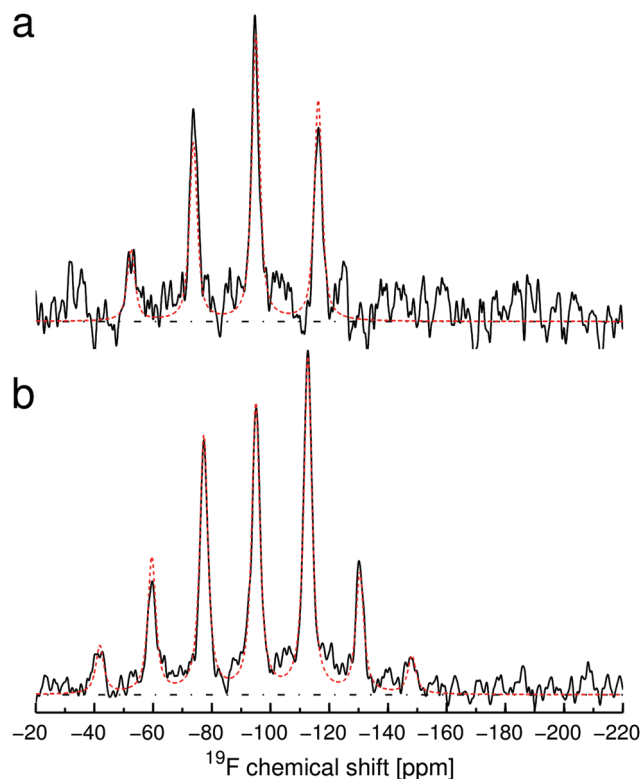
Fig. 4 Solid lines: experimental ^{19}F CP-MAS spectra of 12-F rhodopsin (dark state). Red dashed lines: best-fit results from fitting the chemical shift tensor components. The sample spinning frequency is given by (a) 12 kHz and (b) 10 kHz. The dashed dotted line indicates the baseline.

in good agreement with data reported before for 12-F rhodopsin solubilized in detergent micelles: −94.2 ppm and about +13 ppm, respectively.[53,94] We now show that the large ligation shift rests on very significant shifts in the δ_{22} and δ_{11} chemical shift tensor elements (Tables 2 and 3).

F-NMR analysis of the late photoproducts of 12-F rhodopsin

Analysis of the ^{19}F CP-MAS spectra of the late photoproducts of 12-F rhodopsin shown in Fig. 5 resulted in two sets of resonances with about similar total intensity but differing in centerband linewidth (Table 2). This is expected since in the time required to pack the sample into the rotor slow decay of 12-F Meta II will be proceeding and in the range of 30–50% will have decayed, while the signals of the remaining 12-F rhodopsin and 12-F Meta I are too low to be detectable above the noise level. During the decay of 12-F Meta II, the all-*trans* 12-F-retinal is liberated from the

binding site and then partly diffuses freely in the lipid matrix and partly becomes randomly bound to protein and lipid amino groups.[32] Once the rotors are packed, they are stored and analyzed in a frozen state, which will halt further decay of Meta II. As further outlined in the discussion, we expect that, similar to the difference observed between the free 11-*cis* 12-F-retinoxime and 12-F rhodopsin, the liberated retinal will have a larger linewidth and a smaller anisotropy than the retinal still restricted in the binding site of Meta II. This difference is again observed between the two sets of resonances, and we have assigned them accordingly (Table 2). Since the signal-to-noise ratio in this experiment was not as good as in the rhodopsin analysis, a shorter fully independent second experiment was performed. This corroborated the data of the first experiment ±0.2 ppm for Meta II and ±3 ppm for the liberated retinal. However, it had a much poorer signal-to-noise ratio and therefore only the data of the first experiment have been presented in Table 2.

Table 3 Ligation shifts for the ^{19}F chemical shift tensors upon binding of 11-*cis* 12-F-retinal in rhodopsin and all-*trans* 12-F-retinal in Meta II. Shifts and errors are propagated from Table 2. Data in bold type represent significant differences

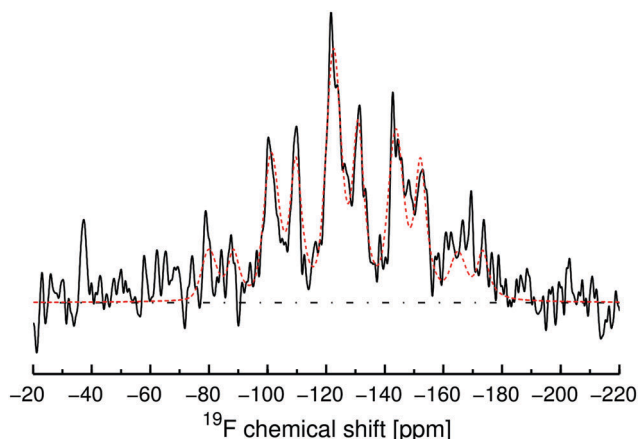| Sample	Ligation shift in chemical shift tensors upon Table 2 (free subtracted from bound)							
	$\Delta\delta_{\text{iso}}$ [ppm]	$\Delta\delta_{\text{aniso}}$ [ppm]	$\Delta\eta$	$\Delta\Omega$ [ppm]	$\Delta\kappa$	$\Delta\delta_{11}$ [ppm]	$\Delta\delta_{22}$ [ppm]	$\Delta\delta_{33}$ [ppm]
Bound *versus* free 11-*cis* 12-F-retinal	**+9.7 ± 0.2**	**+7.1 ± 1.5**	+0.23 ± 0.10	**+18.8 ± 3.5**	+0.20 ± 0.09	**+16.8 ± 1.5**	**+14.3 ± 2.3**	−2.0 ± 2.6
Bound *versus* free all-*trans* 12-F-retinal	**−8.4 ± 0.1**	+4.0 ± 6.3	+0.13 ± 0.20	+11.1 ± 13.4	+0.10 ± 0.16	−4.5 ± 6.3	−5.3 ± 5.1	**−15.5 ± 7.9**

Fig. 5 Solid line: experimental ^{19}F CP-MAS spectrum of illuminated 12-F rhodopsin obtained at 12 kHz sample-spinning frequency. Red dashed lines: best-fit results from fitting the chemical shift tensor components. The dashed dotted line indicates the baseline.

The 12-F Meta II ^{19}F resonance has a linewidth of 2.8 kHz and the analysis of the spinning sideband pattern resulted in isotropic and anisotropic chemical shifts of $\delta_{iso} = -130.9 \pm 0.1$ ppm and $\delta_{aniso} = 54.0 \pm 4.5$ ppm, where the asymmetry parameter is given by $\eta = 1.00 (+0, -0.16)$ (Table 2). This corresponds to a span of $\Omega = 108.1 \pm 9.2$ ppm and a skew of $\kappa = 0.00 \pm 0.06$. The large change in the isotropic ^{19}F chemical shift of -35.9 ppm from the dark-state to the Meta-II state of 12-F rhodopsin is quite noteworthy.

The linewidth of the liberated all-*trans* 12-F-retinal is significantly broader (3.3 kHz). In this case we found an isotropic and anisotropic chemical shift of $\delta_{iso} = -122.5 \pm 0.1$ ppm and $\delta_{aniso} = 50.1 \pm 4.4$ ppm with an asymmetry parameter of $\eta = 0.87 (+0.13, -0.24)$ (Table 2), corresponding to span and skew of $\Omega = 97.0 \pm 9.8$ ppm and $\kappa = -0.10 \pm 0.15$, respectively. These values differ significantly from the ones found for the free 11-*cis* 12-F-retinoxime in liposomes, but the isotropic shift is close to that of all-*trans* 12-F-retinal in CDCl$_3$ solution (-120 ppm) reported before.[49]

We note that the errors in the anisotropic shifts and the asymmetry parameters are significantly larger for 12-F Meta II and liberated all-*trans* 12F-retinal compared to dark-state 12-F rhodopsin and 12-F-retinoxime, as the experiments were solely performed at a single spinning frequency, resulting in less spinning sidebands being used in the analysis. Nevertheless, we find a significant ligation shift (-8.4 ppm) for all-*trans* 12-F-retinal upon binding to the protein, now in the Meta II state, but, remarkably, of opposite sign compared to the ligation shift observed for 11-*cis* 12-F-retinal (Table 3). Also in contrast to 11-*cis* 12-F-retinal, the major contribution to the ligation shift is primarily reflected in the δ_{33} tensor element.

Discussion

We have used a fluorine label at the C12 position of the retinylidene chromophore to probe its environment in the ground state of the rod visual pigment, rhodopsin, and in the activated state,

Meta(rhodopsin) II, by means of solid-state F-NMR. Fluorine labels are quite sensitive NMR-probes, with a broad chemical shift range, and good monitors of their local environment.[44,45] The C12 position was selected for several reasons. First of all, it is part of the photo-active central segment of the chromophore (C-10–C-13) and its vibrational modes strongly support the 11-*cis* to 11-*trans* isomerization and subsequent conformational changes.[10,54–58,60,61,63,64,95] In addition, our previous FTIR study shows significant changes in the vibrational properties of the C12-F derivative in the activated state, but not of the C10-F derivative.[64] Indeed, a preliminary F-NMR study on 10-F labeled octopus rhodopsin indicates small and very similar positive ligation shifts for the rhodopsin and the metarhodopsin state of $+6.4$ and $+4.5$ ppm, respectively.[96] Finally, in contrast to the C12 position, a fluorine label at C11 only shows a very small ligation shift in rhodopsin ($+2$ ppm) and would be very sensitive to bonding partners at C15 that affect the charge distribution over the polyene chain of the chromophore.[49,50,52] This would compromise the interpretation of any changes observed in the activated state, since in rhodopsin the Schiff base linking the chromophore to Lys$_{298}$ in the protein is protonated, but it is unprotonated in Meta II.[1,5,6,19] Furthermore, we have shown before that the 12-F analog of rhodopsin has retained the ability to activate its cognate G-protein transducin following illumination.[64] In conclusion, a fluorine label at the C12 position is most suitable to probe the differences in its microenvironment in rhodopsin and the activated state, Meta II, and correlate this with the available crystal structures.

The isotropic chemical shift we measure for 12-F rhodopsin in a natural membrane environment (-95.0 ppm) agrees very well with the one reported for 12-F rhodopsin in a micellar solution (-94.2 ppm).[53,94] This is not really surprising, since the chromophore is fixed quite tightly in the binding site of the protein and well shielded from solvating molecules.[1,3,8,12,51,97,98] Consequently, the protein micro-environment around the chromophore will be largely unperturbed by the environment the protein is embedded in, as is also evident from the nearly identical spectral properties of rhodopsin in different solvation shells.[1,99]

With respect to the identification of the photoproduct resonances, we have assigned the family of resonances at higher chemical shift to liberated all-*trans* retinal and the set at lower chemical shifts to Meta II. This is based upon the isotropic chemical shift of all-*trans* retinal in organic solvent (-120 ppm), as well as the lower anisotropy and asymmetry parameter together with a larger linewidth for the set at higher chemical shifts, which is also observed for the free 11-*cis* retinoxime relative to the dark-state rhodopsin (Table 2) and likewise is expected for the liberated all-*trans* retinal relative to Meta II. In confirmation, the isotropic chemical shift of the free 11-*cis* and all-*trans* 12-F retinals in our lipid bilayer environment (-104.7 and -122.5 ppm, respectively) is close to the one observed in organic solvents (-107 ppm and -120 ppm, respectively).[49,94]

Clearly, there is a large difference between the isotropic chemical shifts of the 11-*cis* and all-*trans* 12-F retinals in the free state, which can be traced back in all tensor elements (Table 2). Part of this difference is intrinsic to the isomeric state. For instance,

This journal is © the Owner Societies 2018

Phys. Chem. Chem. Phys., 2018, **20**, 30174–30188 | **30181**

there is a 5–10 ppm shift towards higher isotropic chemical shifts of 10-F and 11-F retinal, when going from the all-*trans* to the 9-*cis* and 11-*cis* configuration, respectively.[52,96] The additional positive shift observed for free 12-F retinal in the 11-*cis* configuration probably originates in intramolecular crowding.[100] The 11-*cis* isomer experiences sterical interaction between the C10–H and C13–CH3 elements, which in the free retinal is partially relieved by twisting the C12–C13 bond,[101–103] bringing C12–F and the C13–methyl group in closer contact, which would increase the chemical shift.[94] We find a ±2 ppm difference in the isotropic chemical of the 12-F retinals in a bilayer environment as compared to organic solvent. We would expect a shielding effect of the more hydrophobic lipid acyl chain environment in the bilayer, resulting in a small shift that indeed is observed for the all-*trans* configuration (about −2 ppm). However, the 11-*cis* isomer displays a small shift of about +2 ppm, instead. Currently, we attribute this to stabilization of a special conformation of the curved and twisted 11-*cis* retinal in the acyl chain solvation shell, possibly in combination with intermolecular crowding around the "protruding" C10–C13 structural element. In view of this, the 11-*cis* isomer in organic solvent probably represents a better model of the "free ligand" for estimating protein-induced ligation shifts.

The isotropic chemical shift of the 12-F label, we attribute to the activated state, Meta II, lies at −130.9 ppm, displaying an astonishingly large shift difference of −35.9 ppm from the ground state, rhodopsin. This is almost equally distributed over all principal components of the chemical shift (Table 2), where the differences in each component between the dark and Meta II state are significantly larger than the error of the individual tensor elements. The shift partly originates in the concomitant 11-*cis* to all-*trans* isomerization of the C11=C12 bond, as indicated above, but also stems from the large difference in ligation shift (Table 3).

Such a large shift reflects a significant change in the local environment of the 12-F label upon progressing from the ground state to Meta II. It would be very satisfying if we could link this large shift to the crystal structures of rhodopsin and Meta II.[12,36] This quest is described in the Experimental section and the ESI.† Some relevant data are reported here. First, let us write down eqn (1) in terms of ^{19}F isotropic fluorine chemical shifts:

$$\delta_{iso} = n\delta_{iso}^{F-C} + \delta^{ref} + n^2 A_{iso}^{pol} V^{pol} = -132.58 - 1017.74 V^{pol}$$

$$(2)$$

For an ideal F–C single bond we would obtain $n = 1.0$ and obtain the simple form in the second part of eqn (2). The charge distribution in the binding pocket around the 12-F–C moiety can therefore have two effects: (i) influencing the chemical shift by changing F–C bond length and (ii) causing chemical shift changes by bond polarization.

In our case both rhodopsin models have similar bond C–F bond length and therefore similar values of n: 0.955 for the Meta II state and 0.966 for the dark state. Obviously the value of around −130 ppm, representing the Meta II state, would be reached in situations with low polarization energy V^{pol} where the negative and positive terms in V^{pol} nearly cancel out (see eqn (2)). To reach −95.0 ppm, representing the ground state rhodopsin, the valence must be lower than 1.0—that means a

longer F–C bond—and/or the polarization energy must display large negative values. This will be further elaborated below in the discussion of the CS tensor.

Since most ^{13}C chemical shifts of retinal in rhodopsin and Meta II have been measured and assigned, first a family of structures has been generated linking these shifts with crystal structures (see ESI†). The 20 best structures from this ^{13}C CS refinement are not sufficient for a global minima search for the chromophore with the isotropic ^{19}F chemical shifts of the 12-F as constraints but nevertheless some valuable conclusions could be drawn from these ^{19}F CS calculations (Table 2). At first it can be observed that the trend of the decrease in isotropic chemical shift of the Meta II state is correctly reproduced by the calculations but the total shift was not correctly predicted. It is also noteworthy, that the calculations with a rhodopsin where the carbonyl group of Glu 181 is not protonated perform better than when it is protonated (Table 2).

In going from the dark state to the Meta II state the 33 component is most shifted to negative values (by −41.5 ppm) and the 22 component least shifted (by −31 ppm) and the span increases by 6.4 ppm. This trend is also present in the calculations but the total effect is smaller than in the experiment and the 22 component is shifted into the opposite direction. This is not surprising since the total isotropic shift of the dark state (−95.0 ppm) was not reached in our calculations. Since also the total span is correctly reproduced in our calculations we can conclude that the calculated CS tensor correctly reflects the situation in the two pigments except for an offset. What happens with the CS tensor when the conformation of the retinal is changing is best illustrated in the synthetic powder patterns in Fig. 6. The powder patterns based on the experimentally determined principal
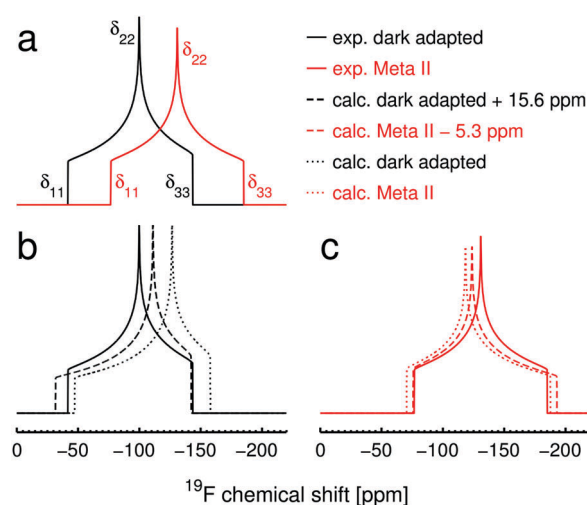
Fig. 6 Synthetic ^{19}F powder patterns for the 12-F retinal pigments: black: dark adapted (rhodopsin) and red: light adapted (Meta II). The principal tensor components are indicated according to Table 1. (a) Comparison of experimental powder patterns for the dark adapted and Meta II state. (b) Comparison of the powder patterns for the dark adapted state based on the experimental and calculated principal components of the chemical shift tensor. (c) Comparison of the powder patterns for Meta II based on the experimental and calculated principal components.

components of the CS tensor for the dark adapted and Meta II state are directly compared in Fig. 6a. Furthermore, Fig. 6b and c compare the powder patterns based on experimentally determined and calculated principal components. We note that if we adjust all calculated principal components by +15.6 ppm for the dark adapted and −5.3 ppm for the Meta II state, we obtain excellent agreement between calculated and experimental powder patterns. See Tables S3 and S4 in the ESI† for details. This indicates that the error in the calculation of the absolute sizes of the principal components is larger than the resulting error in the chemical shift anisotropies that are based on relative sizes. The structural change in the retinal-protein complex is accompanied by a typical change from a negative skew in rhodopsin to a very symmetric powder pattern with skew near zero for the Meta II state. To explain the changes in tensor components it is useful to write down eqn (2) in terms of tensor components (also see Table 1):

$$\begin{pmatrix} \delta_{11}^{F} \\ \delta_{22}^{F} \\ \delta_{33}^{F} \end{pmatrix} = n \begin{pmatrix} -76.98 \\ -117.18 \\ -203.5 \end{pmatrix} + n^2 \begin{pmatrix} -1393.1 \\ 450.8 \\ -2110.8 \end{pmatrix} V^{\text{pol}} \quad (3)$$

The principal tensor components of δ^{F-C} and A^{pol} in eqn (3) can be written as column vectors since the tensor are diagonal within the framework of BPT. Both components δ_{11} and δ_{33} (perpendicular to the bond direction, see Fig. 7) change in such a way that the span of the tensor stays nearly constant (101.7 ppm for rhodopsin and 108.1 ppm for Meta II; Table 2). The higher span of the F bond tensor (126.5 ppm, see Table 1) indicates that the F–C bond is slightly longer ($n < 1.0$) for the retinal in the opsin binding pocket. This can readily derived

Fig. 7 Orientation of calculated ^{19}F chemical shift tensor in the 12-F pigments: (a) the dark adapted state with the 11-*cis* chromophore (rhodopsin). (b) The photo-activated state with all-*trans* chromophore (Meta II). The blue sphere represents the ε-amino group of the protein lysine residue with which the retinal is connected. See also Fig. 8.

from eqn (3) since the configuration weight n acts on all tensor components in the same way.

The change from a very symmetric powder pattern in the case of the Meta II form (skew $\kappa = 0.00$) to a more axial pattern in the case of the dark state (skew $\kappa = -0.15$) can be explained from the different sign of the 22 component of the polarization tensor A^{pol}. That means that the 22 component (in bond direction) is shifted into the opposite field direction with the respect to 11 and 33 by bond polarization (V^{pol} see eqn (3)). We can conclude that the more axial ^{19}F powder pattern of the dark adapted state is caused by large negative polarization energy. In accordance with eqn (3) the largest shift with polarization is calculated for the 33 component because of the large 33 component of A^{pol}.

The orientation of the ^{19}F tensor with respect to the molecular framework could not be extracted from our experiments but for oriented measurements[46] this information is of central interest. As indicated in Fig. 7 the BPT calculations allow assigning the tensor directly to the F–C bond coordinate system. The 22 component of the tensor is in F–C bond direction, the 11 component in the π plane of the sp² carbon 12 and the 33 component perpendicular to it. With this information we can assign the principal tensor components to the bond coordinate system that is used for the definition of C–F bond CS tensor and the CS polarization tensor A^{pol}: the 22 principal component is in z direction, the 11 component in x direction and finally the 33 component in y direction.

The ligation shift we calculate for rhodopsin, *i.e.* the protein induced shift in the chemical shift of its ligand, is a positive shift of +10 to +12 ppm, depending on which reference system is used for the free 11-*cis* ligand. This shift compares well with the *ca.* +13 ppm reported before for rhodopsin solubilized in a micellar environment.[53,94] We here show that this ligation shift mainly originates in large positive shifts in the δ_{11} and δ_{22} tensor elements (Table 2). The ligation shift in rhodopsin has been attributed to steric crowding in the ligand binding site around C12 of the retinylidene moiety.[53] As discussed above, our data indicate that major effects of the binding pocket are elongation and polarization of the 12-F–C bond. Fig. 8 shows the functional groups of the amino acids surrounding the retinal in the binding pocket that are in closest contact to the 12-F site. For the chemical shift optimized structure of the dark-adapted state shown in Fig. 8a we find close contacts of 2.31 and 2.4 Å to the carbonyl groups of Gly-114 and Cys-187, respectively. The oxygen of the closest water molecule is with a distance of 4.21 Å from the 12-F relatively far away.[11,12,92,97] The bond polarization would agree with the strong C–F stretch vibration we observed in 12-F rhodopsin.[64]

The huge difference in isotropic chemical shift of −35.9 ppm, we observe for the activated state, Meta II, relative to the ground state, rhodopsin, has two causes: (i) the 11-*cis* to all-*trans* isomerization shift and (ii) the fact that the ligation shift of the all-*trans* retinal is −8.4 ppm and hence in the opposite direction compared to the 11-*cis* retinal for which it is +9.7 ppm. The ligation shift in Meta II entails a chemical shift decrease, and of a magnitude that is quite unusual upon binding in the
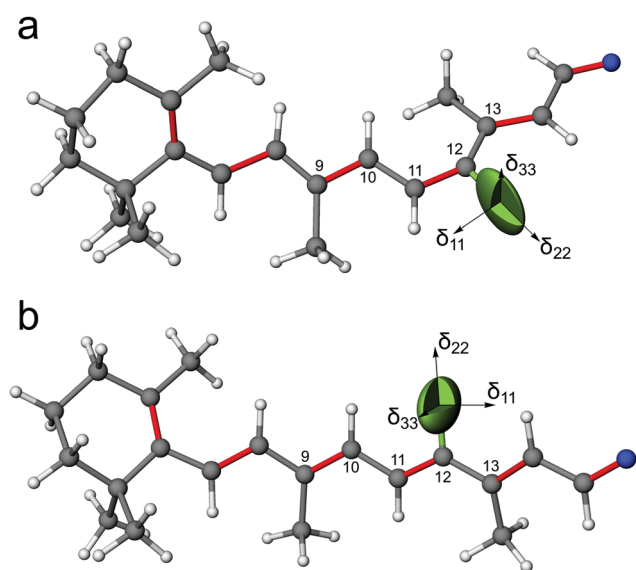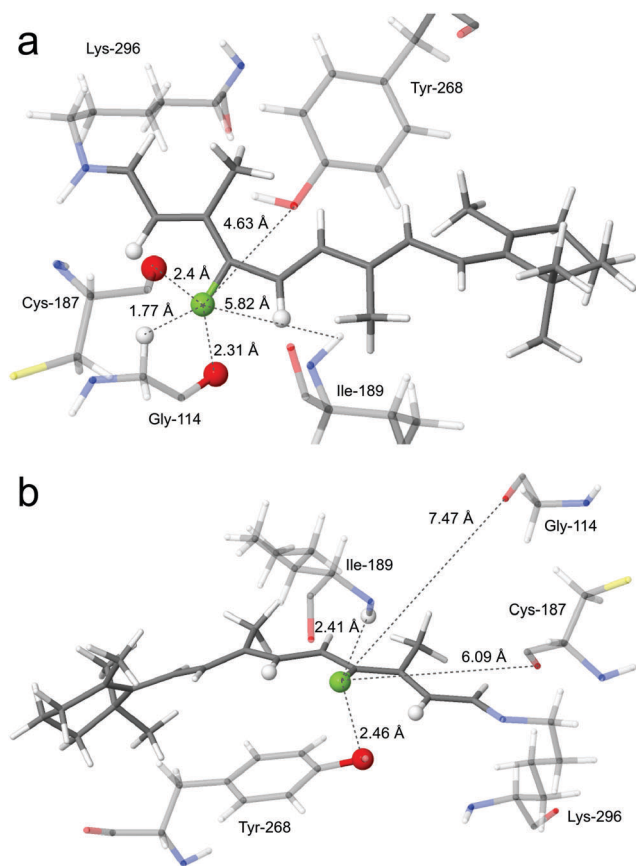
This journal is © the Owner Societies 2018

Phys. Chem. Chem. Phys., 2018, **20**, 30174–30188 | **30183**

Fig. 8 Amino acids in the surrounding of the retinal in the binding pocket in the dark adapted (a) and Meta II form (b) of rhodopsin in chemical shift optimized structures. Contacts of the 12-F (shown in green) mainly responsible for the ^{19}F chemical shift are indicated. In the dark state these are contacts to the oxygen atoms of carbonyl groups of Cys-187 and Gly-144. In the Meta II form these are contacts to the hydrogen atom of the NH group of Ile-189 and the oxygen atom of the hydroxyl group of Tyr-268.

protein interior.[44] In addition, the ligation shift in Meta II is most prominently visible in a very large negative shift in the δ_{33} tensor element (Table 3 and eqn (3)). The BPT calculations provide an explanation together with the chemical shift optimized structure of Meta II shown in Fig. 8b: after the 11-*cis* to all-*trans* transformation of the retinal the 12-F–C bond points in the opposite direction in the binding pocket, hence replacing the close contacts to two carbonyl groups in the dark-state with one close contact to the hydroxyl group of Tyr-268 and one to the amide group of Ile 189 in the Meta II state with distances given by 2.48 Å and 2.41 Å, respectively. The effect of those closest functional groups on the bond polarization cancel each other to a large degree, resulting in a significant decrease of the chemical shift. The slight decrease in bond C–F length and the strong effect on bond polarization, would also explain the slight change in frequency and strong decrease in intensity observed for the C–F stretch vibration.[46] We conclude that the interactions of the retinal with the surrounding binding pocket is strongly reduced in the Meta II state. This is functional, of course, since Meta II has the purpose to mobilize protein structural elements to allow binding of the G protein, and the retinal is about to be released.

Conclusions

Using a ^{19}F label, strategically positioned at C-12 of retinal, the corresponding chemical shift and tensor elements were determined in ground state bovine rhodopsin, its active state photo-intermediate Meta II, and free retinal in a lipid environment. Opposite chemical shifts (+9.7 and −8.4 ppm) were obtained upon binding of the chromophore to obtain rhodopsin and Meta II, respectively. These are due to large changes in the δ_{11} and δ_{22} and in the δ_{33} tensor elements, respectively. An unusually large shift (35.9 ppm) was observed between rhodopsin and Meta II, to which all tensor elements contribute. This shift partly originates in the light-triggered 11-*cis* to all-*trans* isomerization of the chromophore. The other part reflects the local conformational rearrangements in the chromophore and the binding pocket. We set out to correlate these data with the available X-ray structures of rhodopsin and Meta II. However, for this purpose hydrogen atoms have to be inserted and hereto, based upon the X-ray structures, a family of structures was derived that best correlated with the ^{13}C chemical shifts of the chromophores reported in the literature. Following up on these structures, a 12-F derivative was obtained that best corresponds with the ^{19}F chemical shifts and tensor elements that were determined experimentally. The combined data indicate strong changes in the local environment of the C-12 position and a profound change in the interaction pattern of the chromophore with the protein during the transition from rhodopsin to Meta II. We propose, that using alternative ^{19}F-labels on the chromophore as well as selective fluorination of protein residues, in combination with progress in ^{13}C-labeling, will eventually lead to comprehensive structural models and detailed insight in the activation mechanism of visual rhodopsins.

Conflicts of interest

There are no conflicts to declare.

Acknowledgements

References

1 G. Wald, The molecular basis of visual excitation, *Nature*, 1968, **219**(5156), 800–807.
2 O. P. Ernst, K. P. Hofmann and K. Palczewski, Vertebrate rhodopsin, in *Photoreceptors and Light Signalling*, ed. A. Batschauert, Royal Society of Chemistry, Cambridge, 2003, pp. 77–123.

30184 | *Phys. Chem. Chem. Phys.*, 2018, **20**, 30174–30188

This journal is © the Owner Societies 2018

3 K. Palczewski, G protein-coupled receptor rhodopsin, *Annu. Rev. Biochem.*, 2006, **75**, 743–767.

4 M. D. Bownds, Site of attachment of retinal in rhodopsin, *Nature*, 1967, **216**(5121), 1178–1181.

5 H. R. Callender, A. G. Doukas, R. K. Crouch and K. Nakanishi, Molecular flow resonance Raman effect from retinal and rhodopsin, *Biochemistry*, 1976, **15**(8), 1621–1629.

6 R. A. Mathies, A. R. Oseroff and L. Stryer, Rapid-flow resonance Raman spectroscopy of photolabile molecules: rhodopsin and isorhodopsin, *Proc. Natl. Acad. Sci. U. S. A.*, 1976, **73**, 1–5.

7 K. Wang, J. H. McDowell and P. A. Hargrave, Site of attachment of 11-*cis*-retinal in bovine rhodopsin, *Biochemistry*, 1980, **19**(22), 5111–5117.

8 A. F. L. Creemers, S. R. Kiihne, P. H. M. Bovee-Geurts, W. J. DeGrip, J. Lugtenburg and H. J. M. de Groot, ^{1}H and ^{13}C MAS NMR evidence for pronounced ligand-protein interactions involving the ionone ring of the retinylidene chromophore in rhodopsin, *Proc. Natl. Acad. Sci. U. S. A.*, 2002, **99**(14), 9101–9106.

9 M. A. Verhoeven, A. F. L. Creemers, P. H. M. Bovee-Geurts, W. J. DeGrip, J. Lugtenburg and H. J. M. de Groot, Ultra-high-field MAS NMR assay of a multispin labeled ligand bound to its G-protein receptor target in the natural membrane environment: electronic structure of the retinylidene chromophore in rhodopsin, *Biochemistry*, 2001, **40**(11), 3282–3288.

10 M. Carravetta, X. Zhao, O. G. Johannessen, W. C. Lai, M. A. Verhoeven and P. H. M. Bovee-Geurts, *et al.*, Protein-induced bonding perturbation of the rhodopsin chromophore detected by double-quantum solid-state NMR, *J. Am. Chem. Soc.*, 2004, **126**(12), 3948–3953.

11 J. Li, P. C. Edwards, M. Burghammer, C. Villa and G. F. X. Schertler, Structure of bovine rhodopsin in a trigonal crystal form, *J. Mol. Biol.*, 2004, **343**(5), 1409–1438.

12 T. Okada, M. Sugihara, A. N. Bondar, M. Elstner, P. Entel and V. Buss, The retinal conformation and its environment in rhodopsin in light of a new 2.2 Å crystal structure, *J. Mol. Biol.*, 2004, **342**(2), 571–583.

13 M. F. Brown, K. Martínez-Mayorga, K. Nakanishi, G. F. J. Salgado and A. V. Struts, Retinal conformation and dynamics in activation of rhodopsin illuminated by solid-state ^{2}H NMR spectroscopy, *Photochem. Photobiol.*, 2009, **85**(2), 442–453.

14 K. P. Hofmann, Late photoproducts and signaling states of bovine rhodopsin, in *Molecular Mechanisms in Visual Transduction*, ed. D. G. Stavenga, W. J. DeGrip and E. N. J. Pugh, Elsevier Science Pub., Amsterdam, 2000, pp. 91–142.

15 A. Cooper, Energy uptake in the first step of visual excitation, *Nature*, 1979, **282**(5738), 531–533.

16 G. A. Schick, T. M. Cooper, R. A. Holloway, L. P. Murray and R. R. Birge, Energy-storage in the primary photochemical events of rhodopsin and isorhodopsin, *Biochemistry*, 1987, **26**(9), 2556–2562.

17 R. R. Birge and B. W. Vought, Energetics of rhodopsin photobleaching: photocalorimetric studies of energy storage in early and later intermediates, *Methods Enzymol.*, 2000, **315**, 143–163.

18 H. Kühn, Interactions between photoexcited rhodopsin and light-activated enzymes in rods, *Prog. Retinal Res.*, 1984, **3**, 123–156.

19 A. G. Doukas, B. Aton, R. H. Callender and T. G. Ebrey, Resonance Raman studies of bovine metarhodopsin I and metarhodopsin II, *Biochemistry*, 1978, **17**(12), 2430–2435.

20 S. O. Smith, H. J. M. de Groot, R. Gebhard and J. Lugtenburg, Magic angle spinning NMR studies on the metarhodopsin II intermediate of bovine rhodopsin: evidence for an unprotonated Schiff base, *Photochem. Photobiol.*, 1992, **56**(6), 1035–1039.

21 D. L. Farrens, C. A. Altenbach, K. Yang, W. L. Hubbell and H. G. Khorana, Requirement of rigid-body motion of transmembrane helices for light activation of rhodopsin, *Science*, 1996, **274**(5288), 768–770.

22 W. L. Hubbell, C. Altenbach, C. M. Hubbell and H. G. Khorana, Rhodopsin structure, dynamics, and activation: a perspective from crystallography, site-directed spin labeling, sulfhydryl reactivity, and disulfide cross-linking, *Adv. Protein Chem.*, 2003, **63**, 243–290.

23 C. A. Altenbach, A. K. Kusnetzow, O. P. Ernst, K. P. Hofmann and W. L. Hubbell, High-resolution distance mapping in rhodopsin reveals the pattern of helix movement due to activation, *Proc. Natl. Acad. Sci. U. S. A.*, 2008, **105**(21), 7439–7444.

24 H. W. Choe, Y. J. Kim, J. H. Park, T. Morizumi, E. F. Pai and N. Krauß, *et al.*, Crystal structure of metarhodopsin II, *Nature*, 2011, **471**(7340), 651–655.

25 J. Standfuss, P. C. Edwards, A. D'Antona, M. P. Fransen, G. F. Xie and D. D. Oprian, *et al.*, The structural basis of agonist-induced activation in constitutively active rhodopsin, *Nature*, 2011, **471**(7340), 656–660.

26 H. W. Choe, J. H. Park, Y. J. Kim and O. P. Ernst, Transmembrane signaling by GPCRs: Insight from rhodopsin and opsin structures, *Neuropharmacology*, 2011, **60**(1), 52–57.

27 S. Ahuja, V. Hornak, E. C. Y. Yan, N. Syrett, J. A. Goncalves and A. Hirshfeld, *et al.*, Helix movement is coupled to displacement of the second extracellular loop in rhodopsin activation, *Nat. Struct. Mol. Biol.*, 2009, **16**(2), 168–175.

28 S. Ahuja and S. O. Smith, Multiple switches in G protein-coupled receptor activation, *Trends Pharmacol. Sci.*, 2009, **30**(9), 494–502.

29 M. Elgeti, A. S. Rose, F. J. Bartl, P. W. Hildebrand, K. P. Hofmann and M. Heck, Precision vs flexibility in GPCR signaling, *J. Am. Chem. Soc.*, 2013, **135**(33), 12305–12312.

30 Y. Yamazaki, T. Nagata, A. Terakita, H. Kandori, Y. Shichida and Y. Imamoto, Intramolecular interactions that induce helical rearrangement upon rhodopsin activation, *J. Biol. Chem.*, 2014, **289**(20), 13792–13800.

31 E. Malmerberg, P. H. M. Bovee-Geurts, G. Katona, X. Deupi, D. Arnlund and C. Wickstrand, *et al.*, Conformational activation of visual rhodopsin in native disc membranes, *Sci. Signaling*, 2015, **8**(367), ra26.

32 P. J. G. M. van Breugel, P. H. M. Bovee-Geurts, S. L. Bonting and F. J. M. Daemen, Biochemical Aspects of the Visual Process XL. Spectral and chemical analysis of metarhodopsin III in

This journal is © the Owner Societies 2018

Phys. Chem. Chem. Phys., 2018, **20**, 30174–30188 | 30185

photoreceptor membrane suspensions, *Biochim. Biophys. Acta*, 1979, **557**(1), 188–198.

33 K. J. Rothschild, J. Gillespie and W. J. DeGrip, Evidence for rhodopsin refolding during the decay of meta II, *Biophys. J.*, 1987, **51**(2), 345–350.

34 A. L. Klinger and M. S. Braiman, Structural comparison of metarhodopsin II, metarhodopsin III, and opsin based on kinetic analysis of Fourier transform infrared difference spectra, *Biophys. J.*, 1992, **63**(5), 1244–1255.

35 J. Klein-Seetharaman, E. V. Getmanova, M. C. Loewen, P. J. Reeves and H. G. Khorana, NMR spectroscopy in studies of light-induced structural changes in mammalian rhodopsin: applicability of solution 19F NMR, *Proc. Natl. Acad. Sci. U. S. A.*, 1999, **96**(24), 13744–13749.

36 X. Deupi, P. Edwards, A. Singhal, B. Nickle, D. Oprian and G. Schertler, *et al.*, Stabilized G protein binding site in the structure of constitutively active metarhodopsin-II, *Proc. Natl. Acad. Sci. U. S. A.*, 2012, **109**(1), 119–124.

37 K. Palczewski, T. Kumasaka, T. Hori, C. A. Behnke, H. Motoshima and B. A. Fox, *et al.*, Crystal structure of rhodopsin: a G protein-coupled receptor, *Science*, 2000, **289**(5480), 739–745.

38 J. H. Park, P. Scheerer, K. P. Hofmann, H. W. Choe and O. P. Ernst, Crystal structure of the ligand-free G-protein-coupled receptor opsin, *Nature*, 2008, **454**(7201), 183–187.

39 J. J. Ruprecht, T. Mielke, R. Vogel, C. Villa and G. F. X. Schertler, Electron crystallography reveals the structure of metarhodopsin I, *EMBO J.*, 2004, **23**(18), 3609–3620.

40 R. Moukhametzianov, T. Warne, P. C. Edwards, M. J. Serrano-Vega, A. G. W. Leslie and C. G. Tate, *et al.*, Two distinct conformations of helix 6 observed in antagonist-bound structures of a β₁-adrenergic receptor, *Proc. Natl. Acad. Sci. U. S. A.*, 2011, **108**(20), 8228–8232.

41 V. Hornak, S. Ahuja, M. Eilers, J. A. Goncalves, M. Sheves and P. J. Reeves, *et al.*, Light activation of rhodopsin: insights from molecular dynamics simulations guided by solid-state NMR distance restraints, *J. Mol. Biol.*, 2010, **396**(3), 510–527.

42 W. C. Lai, N. McLean, A. Gansmüller, M. A. Verhoeven, G. C. Antonioli and M. Carravetta, *et al.*, Accurate measurements of ^{13}C-^{13}C *J*-couplings in the rhodopsin chromophore by double-quantum solid-state NMR spectroscopy, *J. Am. Chem. Soc.*, 2006, **128**(12), 3878–3879.

43 J. A. Gascón, E. M. Sproviero and V. S. Batista, QM/MM study of the NMR spectroscopy of the retinyl chromophore in visual rhodopsin, *J. Chem. Theory Comput.*, 2005, **1**(4), 674–685.

44 J. T. Gerig, Fluorine NMR of proteins, *Prog. Nucl. Magn. Reson. Spectrosc.*, 1994, **26**(4), 293–370.

45 E. Strandberg, P. Wadhwani, P. Tremouilhac, U. H. N. Dürr and A. S. Ulrich, Solid-state NMR analysis of the PGLa peptide orientation in DMPC bilayers: structural fidelity of ^{2}H-labels versus high sensitivity of ^{19}F-NMR, *Biophys. J.*, 2006, **90**(5), 1676–1686.

46 U. Sternberg, M. Klipfel, S. L. Grage, R. Witter and A. S. Ulrich, Calculation of fluorine chemical shift tensors for the interpretation of oriented 19F-NMR spectra of gramicidin A in membranes, *Phys. Chem. Chem. Phys.*, 2009, **11**(32), 7048–7060.

47 E. V. Getmanova, A. B. Patel, J. Klein-Seetharaman, M. C. Loewen, P. J. Reeves and N. Friedman, *et al.*, NMR spectroscopy of phosphorylated wild-type rhodopsin: mobility of the phosphorylated C-terminus of rhodopsin in the dark and upon light activation, *Biochemistry*, 2004, **43**(4), 1126–1133.

48 M. C. Loewen, J. Klein-Seetharaman, E. V. Getmanova, P. J. Reeves, H. Schwalbe and H. G. Khorana, Solution ^{19}F nuclear Overhauser effects in structural studies of the cytoplasmic domain of mammalian rhodopsin, *Proc. Natl. Acad. Sci. U. S. A.*, 2001, **98**(9), 4888–4892.

49 R. S. H. Liu, M. Denny, J. P. Zingoni, D. Mead, H. Matsumoto and A. E. Asato, Fluorine labeled visual pigments: photoreactivity and ^{19}F-NMR, in *Biophysical Studies of Retinal Proteins*, ed. T. G. Ebrey, H. Frauenfelder, B. Honig and K. Nakanishi, University of Illinois Press, Chicago, 1987, pp. 59–63.

50 R. S. H. Liu and A. E. Asato, The binding site of opsin based on analog studies with isomeric, fluorinated, alkylated, and other modified retinals, in *Chemistry and Biology of Synthetic Retinoids*, ed. M. I. Dawson and W. H. Okamura, CRC Press, Inc., Boca Raton, 1987, pp. 52–75.

51 L. U. Colmenares and R. S. H. Liu, ^{19}F NMR evidence for restricted rotation of the retinyl chromophore in doubly labeled visual pigment analogs, *J. Am. Chem. Soc.*, 1992, **114**(17), 6933–6934.

52 L. U. Colmenares, X. L. Zou, J. Liu, A. E. Asato, R. S. H. Liu and A. R. de Lera, *et al.*, 11,12-Difluororhodopsin and related odd-numbered fluororhodopsins. The use of $J_{F,F}$ for following a *cis-trans* isomerization process, *J. Am. Chem. Soc.*, 1999, **121**(24), 5803–5804.

53 R. S. H. Liu and J. Liu, Fluorinated retinoids and carotenoids, *J. Nat. Prod.*, 2011, **74**(3), 512–517.

54 R. A. Mathies and J. Lugtenburg, The primary photoreaction of rhodopsin. in *Molecular Mechanisms in Visual Transduction*, ed. D. G. Stavenga, W. J. DeGrip and E. N. J. Pugh, Elsevier Science Pub., Amsterdam, 2000, pp. 55–90.

55 P. Kukura, D. W. McCamant, S. Yoon, D. B. Wandschneider and R. A. Mathies, Structural observation of the primary isomerization in vision with femtosecond-stimulated Raman, *Science*, 2005, **310**(5750), 1006–1009.

56 D. Polli, P. Altoè, O. Weingart, K. M. Spillane, C. Manzoni and D. Brida, *et al.*, Conical intersection dynamics of the primary photoisomerization event in vision, *Nature*, 2010, **467**(7314), 440–443.

57 O. Weingart, P. Altoè, M. Stenta, A. Bottoni, G. Orlandi and M. Garavelli, Product formation in rhodopsin by fast hydrogen motions, *Phys. Chem. Chem. Phys.*, 2011, **13**(9), 3645–3648.

58 I. Schapiro, M. N. Ryazantsev, L. M. Frutos, N. Ferré, R. Lindh and M. Olivucci, The ultrafast photoisomerizations of rhodopsin and bathorhodopsin are modulated by bond length alternation and HOOP driven electronic effects, *J. Am. Chem. Soc.*, 2011, **133**(10), 3354–3364.

30186 | *Phys. Chem. Chem. Phys.*, 2018, **20**, 30174–30188

This journal is © the Owner Societies 2018

59 P. J. M. Johnson, A. Halpin, T. Morizumi, V. I. Prokhorenko, O. P. Ernst and R. J. D. Miller, Local vibrational coherences drive the primary photochemistry of vision, *Nat. Chem.*, 2015, **7**(12), 980–986.

60 C. Schnedermann, M. Liebel and P. Kukura, Mode-specificity of vibrationally coherent internal conversion in rhodopsin during the primary visual event, *J. Am. Chem. Soc.*, 2015, **137**(8), 2886–2891.

61 C. Schnedermann, X. Yang, M. Liebel, K. M. Spillane, J. Lugtenburg and I. Fernández, *et al.*, Evidence for a vibrational phase-dependent isotope effect on the photo-chemistry of vision, *Nat. Chem.*, 2018, **10**(4), 449–455.

62 F. DeLange, P. H. M. Bovee-Geurts, A. M. A. Pistorius, K. J. Rothschild and W. J. DeGrip, Probing intramolecular orientations in rhodopsin and metarhodopsin II by polarized infrared difference spectroscopy, *Biochemistry*, 1999, **38**(40), 13200–13209.

63 A. V. Struts, G. F. J. Salgado, K. Martínez-Mayorga and M. F. Brown, Retinal dynamics underlie its switch from inverse agonist to agonist during rhodopsin activation, *Nat. Struct. Mol. Biol.*, 2011, **18**(3), 392–394.

64 P. H. M. Bovee-Geurts, I. Fernández Fernández, R. S. H. Liu, R. A. Mathies, J. Lugtenburg and W. J. DeGrip, Fluoro derivatives of retinal illuminate the decisive role of the C_{12}-H element in photoisomerization and rhodopsin activation, *J. Am. Chem. Soc.*, 2009, **131**(49), 17933–17942.

65 R. S. H. Liu, H. Matsumoto, A. E. Asato, M. Denny, Y. Shichida and T. Yoshizawa, *et al.*, Synthesis and properties of 12-fluororetinal and 12-fluororhodopsin. A model system for ^{19}F NMR studies of visual pigments, *J. Am. Chem. Soc.*, 1981, **103**(24), 7195–7201.

66 F. DeLange, P. H. M. Bovee-Geurts, J. VanOostrum, M. D. Portier, P. J. E. Verdegem and J. Lugtenburg, *et al.*, An additional methyl group at the 10-position of retinal dramatically slows down the kinetics of the rhodopsin photocascade, *Biochemistry*, 1998, **37**(5), 1411–1420.

67 W. J. DeGrip, J. VanOostrum, P. H. M. Bovee-Geurts, R. van der Steen, L. J. P. VanAmsterdam and M. Groesbeek, *et al.*, 10,20-Methanorhodopsins: (7E,9E,13E)-10,20-methano-rhodopsin and (7E,9Z,13Z)-10,20-methanorhodopsin—11-*cis*-Locked rhodopsin analog pigments with unusual thermal and photo-stability, *Eur. J. Biochem.*, 1990, **191**(1), 211–220.

68 W. J. DeGrip, J. VanOostrum and P. H. M. Bovee-Geurts, Selective detergent-extraction from mixed detergent/lipid/protein micelles, using cyclodextrin inclusion compounds: a novel generic approach for the preparation of proteolipo-somes, *Biochem. J.*, 1998, **330**(2), 667–674.

69 F. DeLange, M. Merkx, P. H. M. Bovee-Geurts, A. M. A. Pistorius and W. J. DeGrip, Modulation of the metarhodopsin I/metarhodopsin II equilibrium of bovine rhodopsin by ionic strength—Evidence for a surface charge effect, *Eur. J. Biochem.*, 1997, **243**(1-2), 174–180.

70 P. J. R. Spooner, J. M. Sharples, S. C. Goodall, P. H. M. Bovee-Geurts, M. A. Verhoeven and J. Lugtenburg, *et al.*, The ring of the rhodopsin chromophore in a hydrophobic activation switch within the binding pocket, *J. Mol. Biol.*, 2004, **343**(3), 719–730.

71 E. O. Stejskal, J. Schaefer and J. S. Waugh, Magic-angle spinning and polarization transfer in proton-enhanced NMR, *J. Magn. Reson.*, 1977, **28**(1), 105–112.

72 E. L. Hahn, Spin echoes, *Phys. Rev.*, 1950, **80**(4), 580–594.

73 R. K. Harris, E. D. Becker, S. M. De Menezes, P. Granger, R. E. Hoffman and K. W. Zilm, Further conventions for NMR shielding and chemical shifts (IUPAC recommendations 2008), *Pure Appl. Chem.*, 2008, **80**(1), 59–84.

74 C. P. Rosenau, B. J. Jelier, A. D. Gossert and A. Togni, Exposing the origins of irreproducibility in fluorine NMR spectroscopy, *Angew. Chem., Int. Ed.*, 2018, **57**(30), 9528–9533.

75 A. Bielecki and D. P. Burum, Temperature dependence of ^{207}Pb MAS spectra of solid lead nitrate. An accurate, sensitive thermometer for variable-temperature MAS, *J. Magn. Reson., Ser. A*, 1995, **116**(2), 215–220.

76 M. Concistrè, A. Gansmüller, N. McLean, O. G. Johannessen, I. M. Montesinos and P. H. M. Bovee-Geurts, *et al.*, Double-quantum ^{13}C nuclear magnetic resonance of bathorhodopsin, the first photointermediate in mammalian vision, *J. Am. Chem. Soc.*, 2008, **130**(32), 10490–10491.

77 A. Detken, E. H. Hardy, M. Ernst and B. H. Meier, Simple and efficient decoupling in magic-angle spinning solid-state NMR: the XiX scheme, *Chem. Phys. Lett.*, 2002, **356**(3-4), 298–304.

78 U. Haeberlen, in *High Resolution NMR in Solids. Selective Averaging*, ed. J. S. Waugh, Academic Press, New York, 1976.

79 C. J. Jameson, Reply to conventions for tensor quantities used in nuclear magnetic resonance, nuclear quadrupole resonance and electron spin resonance spectroscopy, *Solid State Nucl. Magn. Reson.*, 1998, **11**(3), 265–268.

80 O. N. Antzutkin, Sideband manipulation in magic-angle-spinning nuclear magnetic resonance, *Prog. Nucl. Magn. Reson. Spectrosc.*, 1999, **35**(3), 203–266.

81 M. Edén and H. Levitt, Computation of orientational averages in solid-state NMR by Gaussian spherical quad-rature, *J. Magn. Reson.*, 1998, **132**(2), 220–239.

82 G. A. F. Seber and C. J. Wild, *Nonlinear Regression*, Wiley-Interscience, Hoboken, 2003.

83 E. M. L. Beale, Confidence Regions in Non-Linear Estimation, *J. R. Stat. Soc. Series B Stat. Methodol.*, 1960, **22**(1), 41–88.

84 R. Witter, M. Möllhoff, F. T. Koch and U. Sternberg, Fast atomic charge calculation for implementation into a polarizable force field: application to an ion channel protein, *J. Chem.*, 2015, **2015**, 908204.

85 I. Jakovkin, M. Klipfel, C. Muhle-Goll, A. S. Ulrich, B. Luy and U. Sternberg, Rapid calculation of protein chemical shifts using bond polarization theory and its application to protein structure refinement, *Phys. Chem. Chem. Phys.*, 2012, **14**(35), 12263–12276.

86 M. Schindler, *Die Berechnung magnetischer Eigenschaften unter Verwendung individuell geeichter lokalisierter Molekülorbitale*, PhD thesis, Ruhr-University Bochum, Bochum, 1980.

87 L. Pauling, *The Nature of the Chemical Bond*, Cornell University Press, Ithaca, 3rd edn, 1960.

88 M. O'Keefe and N. E. Breese, Atom sizes and bond lengths in molecules and crystals, *J. Am. Chem. Soc.*, 1991, **113**(9), 3226–3229.

This journal is © the Owner Societies 2018

Phys. Chem. Chem. Phys., 2018, **20**, 30174–30188 | **30187**

89 R. Witter, W. Prieß and U. Sternberg, Chemical shift driven geometry optimization, *J. Comput. Chem.*, 2002, **23**(2), 298–305.

90 M. Möllhoff and U. Sternberg, Molecular mechanics with fluctuating atomic charges—a new force field with a semi-empirical charge calculation, *J. Mol. Model.*, 2001, **7**(4), 90–102.

91 U. Sternberg, F. T. Koch, M. Bräuer, M. Kunert and E. Anders, Molecular mechanics for zinc complexes with fluctuating atomic charges, *J. Mol. Model.*, 2001, **7**, 54–64.

92 J. S. Frähmcke, M. Wanko, P. Phatak, M. A. Mroginski and M. Elstner, The protonation state of Glu181 in rhodopsin revisited: interpretation of experimental data on the basis of QM/MM calculations, *J. Phys. Chem. B*, 2010, **114**(34), 11338–11352.

93 U. H. N. Dürr, S. L. Grage, R. Witter and A. S. Ulrich, Solid state ^{19}F NMR parameters of fluorine-labeled amino acids. Part I: aromatic substituents, *J. Magn. Reson.*, 2008, **191**, 7–15.

94 R. S. H. Liu and L. U. Colmenares, ^{19}F-NMR in studies of fluorinated visual pigment analogs. A method for detecting neighbouring groups or empty space in a binding site, in *Structures and functions of retinal proteins*, ed. J. L. Rigaud, INSERM-John Libbey Eurotext Ltd, London, 1992, pp. 251–254.

95 M. A. Verhoeven, P. H. M. Bovee-Geurts, H. J. M. de Groot, J. Lugtenburg and W. J. DeGrip, Methyl substituents at the 11- or 12-position of retinal profoundly and differentially affect photochemistry and signalling activity of rhodopsin, *J. Mol. Biol.*, 2006, **363**(1), 98–113.

96 T. Iwasa, L. U. Colmenares, K. Hirata, Y. Arime, M. Nakagawa and S. Kikkawa, *et al.*, ^{19}F-NMR and UV-Vis absorption spectroscopic studies of fluorinated octopus rhodopsin and its photoproducts, *J. Phys. Chem. A*, 1998, **102**(28), 5602–5610.

97 B. Jastrzebska, K. Palczewski and M. Golczak, Role of bulk water in hydrolysis of the rhodopsin chromophore, *J. Biol. Chem.*, 2011, **286**(21), 18930–18937.

98 K. Nakanishi and R. K. Crouch, Application of artificial pigments to structure determination and study of photoinduced transformations of retinal proteins, *Isr. J. Chem.*, 1995, **35**(3–4), 253–272.

99 H. Motoyama, T. Hamanaka, Y. Kito, H. Morita, L. Guerette and D. Abran, *et al.*, Wavelength modulation by molecular environment in visual pigments, *Biochim. Biophys. Acta*, 1986, **861**, 9–15.

100 G. W. Gribble, D. J. Keavy, E. R. Olson, I. D. Rae, A. Staffa and T. E. Herr, *et al.*, Fluorine deshielding in the proximity of a methyl-group. An experimental and theoretical study, *Magn. Reson. Chem.*, 1991, **29**(5), 422–432.

101 M. Han and S. O. Smith, NMR constraints on the location of the retinal chromophore in rhodopsin and bathorhodopsin, *Biochemistry*, 1995, **34**(4), 1425–1432.

102 X. Feng, P. J. E. Verdegem, Y. K. Lee, D. Sandström, M. Edén and P. H. M. Bovee-Geurts, *et al.*, Direct determination of a molecular torsional angle in the membrane protein rhodopsin by solid-state NMR, *J. Am. Chem. Soc.*, 1997, **119**(29), 6853–6857.

103 A. Bifone, H. J. M. de Groot and F. Buda, Ab initio molecular dynamics of rhodopsin, *Pure Appl. Chem.*, 1997, **69**(10), 2105–2110.